and fig. S12). This result—less variability when varves are thicker—indicates reduced variability in East African winds and rainfall at ENSO time scales under cold LGM conditions. It is notable that the late Holocene sediments, characterized by thinner varves on average, nevertheless have the thickest individual varves (Fig. 3). Thus, although the interglacial is generally characterized by wetter, less windy conditions, it has experienced years that were windier (and thus very likely also drier) than prevailed during the last ice age (*23*).

These findings of a more interannually stable climate in East Africa during colder periods support the notion of the strong sensitivity of the winds and the hydrological cycle to the larger-scale climate. Warmer climate states appear to produce greater climate variability. This inference fits the growing consensus that current global warming will intensify the hydrological cycle, with wet regions and periods becoming wetter and dry regions and periods becoming drier (*24*). As an example of this tendency from models, experiments with the National Center for Atmospheric Research (NCAR) Community Climate Systems Model (CCSM3) coupled the general circulation model for LGM, preindustrial and modern conditions, and a doubling of preindustrial CO_2 levels (*25*, *26*) show the same trends in mean rainfall and rainfall variability in eastern equatorial Africa in relation to mean temperatures as indicated by our lake varve data (Fig. 3): Under warmer climates, both mean rainfall and interannual rainfall variability are greater (Fig. 3A). A future increase in the interannual variability of rainfall in equatorial eastern Africa, which is projected by the model and supported by our varve thickness data, may bring further environmental stress to a region with a reduced capacity to adapt to the mounting adverse effects of global climate change.

References and Notes

1. M. L. Parry, Intergovernmental Panel on Climate Change Working Group II, Eds., *Climate Change 2007: Impacts, Adaptation and Vulnerability: Contribution of Working Group II to the Fourth Assessment Report of the Intergovernmental Panel on Climate Change* (Cambridge Univ. Press, Cambridge, 2007).
2. S. E. Nicholson, in *The Limnology, Climatology and Paleoclimatology of the East African Lakes,* T. C. Johnson, E. O. Odada, Eds. (Gordon & Breach, Amsterdam, 1996), pp. 25–56.
3. S. E. Nicholson, *Global Planet. Change* **26**, 137 (2000).
4. C. F. Ropelewski, M. S. Halpert, *Mon. Weather Rev.* **115**, 1606 (1987).
5. M. Latif, D. Dommenget, M. Dima, A. Grötzner, *J. Clim.* **12**, 3497 (1999).
6. L. Goddard, N. E. Graham, *J. Geophys. Res.* **104**, (D16), 19099 (1999).
7. N. H. Saji, B. N. Goswami, P. N. Vinayachandran, T. Yamagata, *Nature* **401**, 360 (1999).
8. E. Black, J. Slingo, K. R. Sperber, *Mon. Weather Rev.* **131**, 74 (2003).
9. S. Hastenrath, D. Polzin, *Q. J. R. Meteorol. Soc.* **130**, 503 (2004).
10. D. Verschuren *et al.*, *Nature* **462**, 637 (2009).
11. C. H. Pilskaln, T. C. Johnson, *Limnol. Oceanogr.* **36**, 544 (1991).
12. A. Kaplan *et al.*, *J. Geophys. Res.* **103**, (C9), 18567 (1998).
13. N. A. Rayner *et al.*, *J. Geophys. Res. Atmos.* **108**, (D14), 4407 (2003).
14. J. Moernaut *et al.*, *Earth Planet. Sci. Lett.* **290**, 214 (2010).
15. P. U. Clark *et al.*, *Science* **325**, 710 (2009).
16. D. Verschuren, K. R. Laird, B. F. Cumming, *Nature* **403**, 410 (2000).
17. G. H. Haug, K. A. Hughen, D. M. Sigman, L. C. Peterson, U. Rohl, *Science* **293**, 1304 (2001).
18. G. N. Kiladis, H. F. Diaz, *J. Clim.* **2**, 1069 (1989).
19. C. M. Moy, G. O. Seltzer, D. T. Rodbell, D. M. Anderson, *Nature* **420**, 162 (2002).
20. F. Gasse, F. Chalie, A. Vincens, M. A. J. Williams, D. Williamson, *Quat. Sci. Rev.* **27**, 2316 (2008).
21. C. Sonzogni, E. Bard, F. Rostek, *Quat. Sci. Rev.* **17**, 1185 (1998).
22. F. Justino, W. R. Peltier, *J. Clim.* **21**, 459 (2008).
23. D. McGee, W. S. Broecker, G. Winckler, *Quat. Sci. Rev.* **29**, 2340 (2010).
24. I. M. Held, B. J. Soden, *J. Clim.* **19**, 5686 (2006).
25. S. G. Yeager, C. A. Shields, W. G. Large, J. J. Hack, *J. Clim.* **19**, 2545 (2006).
26. B. L. Otto-Bliesner *et al.*, *J. Clim.* **19**, 2526 (2006).
27. E. Kalnay *et al.*, *Bull. Am. Meteorol. Soc.* **77**, 437 (1996).
28. S. O. Rasmussen *et al.*, *J. Geophys. Res. Atmos.* **111**, (D6), D06102 (2006).
29. E. C. Hopmans *et al.*, *Earth Planet. Sci. Lett.* **224**, 107 (2004).

Acknowledgments: This work received funding from the European Science Foundation EUROCORES program EuroCLIMATE [Framework Programme 28: Lake Challa: a Long Archive of Climate in Equatorial Africa (CHALLACEA)] and through the Graduate School GRK 1364 Shaping Earth's Surface in a Variable Environment funded by the DFG. C.W. is grateful for grant from Leibniz Center for Earth Surface Process and Climate Studies. A.T. received support from NSF grant AGS-1010869 and the Japan Agency for Marine-Earth Science and Technology (JAMSTEC). Fieldwork was conducted with research permission of the Kenyan Ministry of Education and Science to D.V. (MOEST 13/001/11C). We gratefully acknowledge C. M. Oluseno, I. Kristen, U. Frank, and A. Hoechner for comments and assistance and the CHALLACEA team for stimulating discussions. This is IPRC publication no. 805.

Supporting Online Material

www.sciencemag.org/cgi/content/full/333/6043/743/DC1
Materials and Methods
Figs. S1 to S12
Table S1
References

2 February 2011; accepted 17 June 2011
10.1126/science.1203724

A 10,000-Year Record of Arctic Ocean Sea-Ice Variability—View from the Beach

Svend Funder,[1]* Hugues Goosse,[2] Hans Jepsen,[1] Eigil Kaas,[3] Kurt H. Kjær,[1] Niels J. Korsgaard,[1] Nicolaj K. Larsen,[4] Hans Linderson,[5] Astrid Lysså,[6] Per Möller,[5] Jesper Olsen,[7] Eske Willerslev[1]

We present a sea-ice record from northern Greenland covering the past 10,000 years. Multiyear sea ice reached a minimum between ~8500 and 6000 years ago, when the limit of year-round sea ice at the coast of Greenland was located ~1000 kilometers to the north of its present position. The subsequent increase in multiyear sea ice culminated during the past 2500 years and is linked to an increase in ice export from the western Arctic and higher variability of ice-drift routes. When the ice was at its minimum in northern Greenland, it greatly increased at Ellesmere Island to the west. The lack of uniformity in past sea-ice changes, which is probably related to large-scale atmospheric anomalies such as the Arctic Oscillation, is not well reproduced in models. This needs to be further explored, as it is likely to have an impact on predictions of future sea-ice distribution.

Global warming will probably cause the disappearance of summer sea ice in the Arctic Ocean during this century (*1*,*2*), and the ocean bordering North Greenland is expected to be the very last area to become ice-free in summer (*2*–*4*). We present a long-term (~10,000-year) record of variations in multiyear and land-fast sea ice from this key area, using the abundance and origin of driftwood as signals of multiyear sea ice and its traveling route, and the occurrence or absence of beach ridges as signals of seasonally open water. This record is compared with a previously published record from the western Arctic Ocean, which is based on the same type of evidence and is sensitive to the same oceanographic and climatic factors (*5*-*7*).

Driftwood on Greenland's raised beaches and shores originates from transocean drift from Asia and America. The voyage takes several

[1]Centre for GeoGenetics, Natural History Museum of Denmark, University of Copenhagen, Øster Voldgade 5-7, DK 1350 Copenhagen K, Denmark. [2]Université Catholique de Louvain, Earth and Life Institute, Centre de Recherches sur la Terre et le Climat Georges Lemaître, Chemin du Cyclotron, 2, 1348, Louvain-la-Neuve, Belgium. [3]Niels Bohr Institute, University of Copenhagen, Juliane Maries Vej 30, DK 2100 Copenhagen, Denmark. [4]Geological Institute University of Aarhus, C. F. Møllers Allé 4, DK 8000 Aarhus C, Denmark. [5]GeoBiosphere Science Centre, Quaternary Sciences, Lund University, Sölvegatan 12, SE 22362 Lund, Sweden. [6]Geological Survey of Norway, 7491 Trondheim, Norway. [7]School of Geography, Archaeology and Palaeoecology, Queen's University, Belfast, Belfast BT7 1NN, UK.

*To whom correspondence should be addressed. E-mail: svf@snm.ku.dk

years and can only be accomplished if the wood is incorporated in sea ice at the onset (*8*). The driftwood in Greenland is therefore an indicator of multiyear pack ice. We collected, identified, and dated (using ^{14}C accelerator mass spectrometry) driftwood from a stretch of 500 km of the northern coast (Fig. 1 and fig. S1). The abundance of driftwood on Greenland's shores is determined by various factors during the voyage across the ocean (*9*, *10*) but also by land-fast ice, which blocks the landing of driftwood and is controlled by local temperatures and wind (*9*). The most direct route for the transportation of driftwood to Greenland is from central Siberia on the Transpolar Drift (TPD), with a travelling time of 2 to 5 years (*11*, *12*), carrying mainly larch (*Larix*), which dominates north Siberian forests (Fig. 2B) (*6*, *13*). The voyage from North America is more precarious because the wood has to go into the Beaufort Gyre (BG) and make a detour around Siberia before it can join the TPD, increasing the traveling time to 6 to 7 years or more (Fig. 2B) (*11*, *12*) and signified by spruce (*Picea*), which dominates the boreal forest in North America (*6*, *13*). The changing proportions of larch and spruce therefore indicate changes in the strength of the TPD and BG, which are driven by atmospheric circulation (*6*, *11*).

In order to determine the absence or presence of year-round land-fast ice, we mapped the occurrence of beach ridge complexes along the coast (Fig. 3 and table S3) (*10*). Beach ridges are formed by wave transportation and sorting of sediment on dissipative platforms with an adequate supply of sediments (*14*). The coastal plain bordering the Arctic Ocean from Greenland's northern tip and several hundred kilometers to the southeast is the platform for dissipative beaches, and its cover of unconsolidated sediment provides sediment for waves to work on. Currently, no beach ridges are formed along these coasts, owing to the damping effect of the sea ice (fig. S1), and the raised beach ridge complexes therefore indicate periods with more open water along the coast than now. To the south, the ridges are long (>10 km) and occur in all suitable areas (table S3), signifying seasonally open water along the coast (Fig. 3, areas 2 to 5; and fig. S1). North of 83°, the ridges become short and occur only at the mouths of major valleys and embayments (Fig. 3 and fig. S1), and the terrain surface between areas with beach ridge complexes is a barren plain of fine-grained marine sediment without traces of wave action (fig. S1). At higher levels, pebbles and striated boulders form a deflation lag on the windswept surface of the plain (fig. S1). This shows that the coast was permanently blocked by ice but with coastal melt in areas with concentrated runoff from land. The boulders show that icebergs were free to move along the coast and were not inhibited by long-lasting land-fast ice, as at present (Fig. 2, area 1; and fig. S1) (*15*). We dated the beach ridges by their history of isostatic uplift as shown in relative sea level (RSL) curves for five different areas along the coast, based on ^{14}C dates of marine molluscs and other organic matter (Fig. 3 and table S2) (*10*).

Combining the driftwood and beach ridge evidence, we distinguish four main phases in the development of sea ice in this part of the Arctic Ocean (Fig. 1). (i) Deglaciation of the coastal plain at ~10 thousand years before the present (ky B.P.) was followed by marine transgression (*16*). Until ~8.5 ky B.P., there was only sporadic driftwood, and beach ridges occurred only at the southernmost locality. On Ellesmere Island, in a similar environment (*5*), abundant driftwood shows that its absence in northern Greenland is not because of preservation issues, and the large boulders on the plains of marine sediment suggest that icebergs from local glaciers blocked the access of pack ice to the coast. (ii). The period ~8.5 to 6 ky B.P. marks the Holocene Thermal Maximum (HTM) in this area. Long continuous beach ridges northward along the coast up to 83°N show that this was the southern limit of permanent sea ice, ~1000 km to the north of its present position (Fig. 1C). To the north of 83°N,

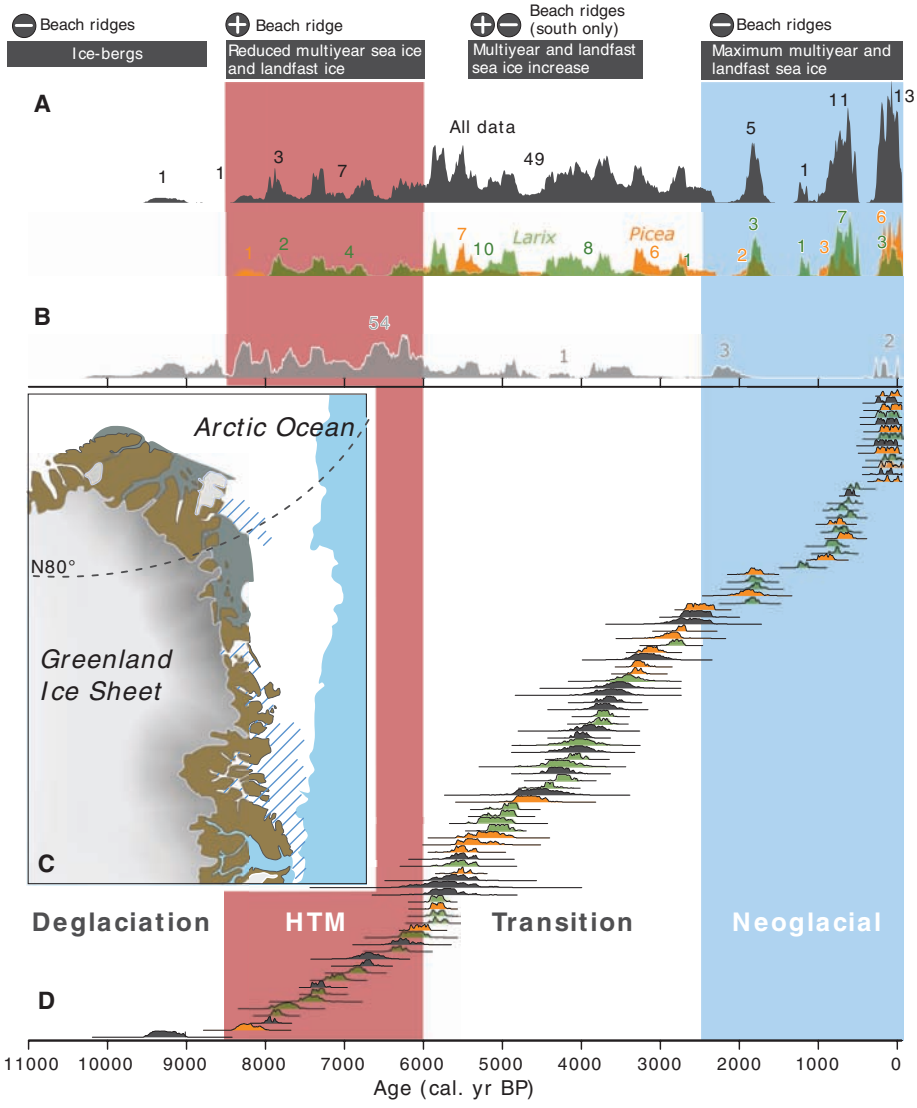

Fig. 1. Driftwood dates and sea-ice conditions in northeast Greenland. (**A**) Cumulative calibrated probability distributions (CPDs) of calibrated ^{14}C ages on driftwood from Greenland north of 80°N (black), of *Picea* (spruce, orange) and *Larix* (larch, green) from North Greenland, and (**B**) from northern Ellesmere Island (gray, from (*5*)]. Because probabilities cannot be directly summed, the number of dates within each date block is shown by figures. (**C**) Summer sea ice along the coast of Greenland at the September 2007 Arctic record minimum. Gray, landfast ice; white, pack ice (>20% coverage); blue-striped area, coastal melt (<20% coverage, including the Northeast Water Polynya). In late September, the land-fast ice was swept away, and until late November, the north coast was exposed to dense pack ice—a situation that has characterized the past decade (*26*). (**D**) CPD on single pieces of north Greenland driftwood. Black, unidentified; other colors as above. ^{14}C dates have been calibrated with OxCal 4.1, using the intcal09 calibration curve, and are shown with 95% probability distributions (*27*, *28*) (table S1) (*10*).

beach ridges are restricted to bays and major river mouths, showing that this coast had permanent sea ice but was within the zone of coastal melt (Fig. 1C). Coastal melt is determined by local summer temperatures (*15*), and this indicates that summer temperatures during the HTM in north Greenland were 2° to 4°C warmer than now, as elsewhere in this part of the Arctic (*17*). Driftwood from this period is sparse, and because there was free access to the coast, we can conclude that multiyear sea ice was reduced. Although driftwood was sparse in Greenland, near-

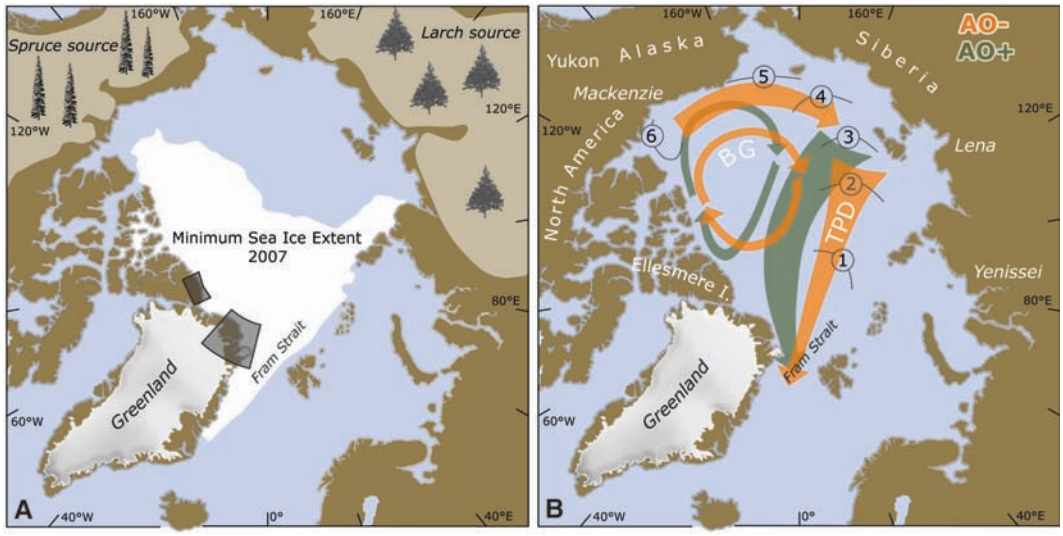

Fig. 2. The Arctic Ocean with (**A**) working area in northeast Greenland and the area for driftwood dates from Ellesmere Island [from (*5*)]; main source areas for Greenland driftwood, with the present distribution of larch and spruce (*10*); and record low summer sea-ice distribution in September 2007 [>15% coverage, (*1*)]. (**B**) Surface currents in the Arctic Ocean during periods of AO+ and AO− situations [from (*23*)] and travel route and time for sea ice in the Arctic Ocean (years to reach Fram Strait) [from (*12*)].

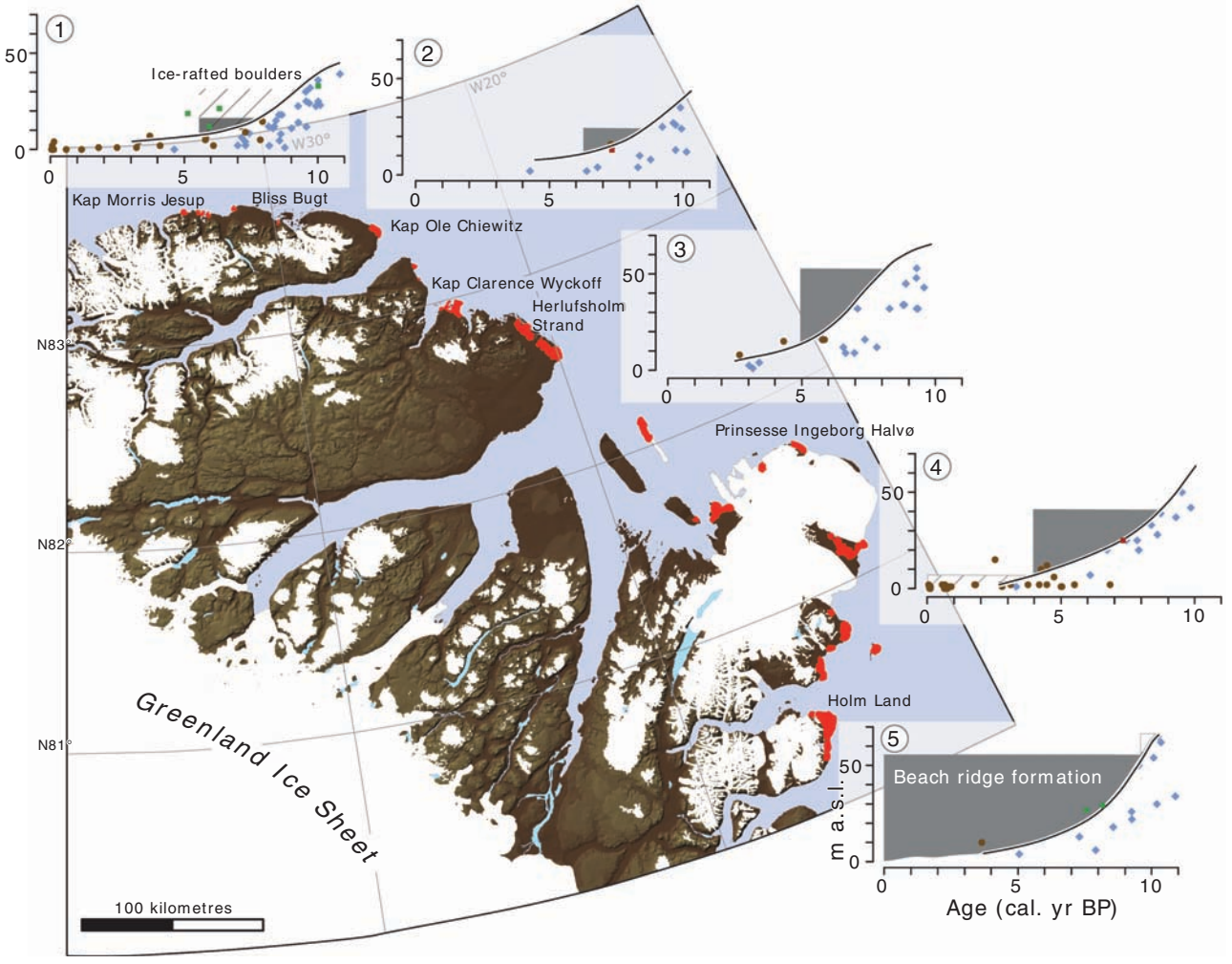

Fig. 3. Northeast Greenland beach ridge complexes and their dating. Red, areas of beach ridge complexes. (**Insets**) RSL curves with dating of the period of beach ridge formation in each area (dark gray shading). The curves are based on ^{14}C dates from the following: blue, bivalve shells; brown, driftwood; green, terrestrial plants. Red, lake isolation date (fig. S2 and tables S1 and S2).

by Ellesmere Island experienced a boom (*5*), as discussed below (Fig. 1A). (iii) After 6 ky B.P., there is a sudden rise in driftwood, and beach ridge formation is restricted to the southern areas, showing that periods of open water became shorter from ~5.5 ky B.P. Nevertheless, our data suggest more open water than at present until at least 4.5 ky B.P. (Fig. 3). The same pattern is seen on Ellesmere Island, but here permanent land-fast ice began to grow at 5.5 ky B.P., spreading to block most of the coast at 3.5 ky B.P. (*5*). From ~6 ky B.P., spruce became a steady component of the driftwood in Greenland. This indicates that after a sudden start, a change to more frequent situations with a strong BG began, increasing the transport of American sea ice to Greenland. Further south on East Greenland's coast, as well as at Iceland and Svalbard, sea ice emanating from the Arctic Ocean also increased after 7 ky B.P. and especially after ~5 ky B.P. (*13*, *18*–*21*) (Fig. 1C). (iv). At ~2.5 ky B.P., an era of dramatic centennial fluctuations in driftwood abundance and of change of source areas began. This period comprises half of our driftwood finds, but the high frequencies are punctuated by woodless periods at 2.5 to 2 ky B.P., 1.7 to 0.9 ky B.P., 0.5 to 0.3 ky B.P., and probably since ~1950. The lack of beach ridges shows that the coast was blocked by ice, and the woodless intervals signify perennial land-fast ice. The intervening intervals with high driftwood incidence show varying dominance of spruce and larch. A larch-dominated peak at ~1100 to 1400 indicates a strong TPD and a weak BG during the Medieval Warm Period, whereas the woodless periods and the increase in spruce after 1400 show that situations with large BG input became increasingly frequent during the Little Ice Age (LIA), as shown also in the western Arctic Ocean (*22*).

As noted above, during the HTM, when driftwood was sparse in Greenland, it boomed on Ellesmere Island, 600 km to the southwest (Fig. 1A) (*5*). In Greenland, the driftwood is almost entirely larch from Siberia, whereas spruce dominated on Canada's Arctic Ocean coast until ~7.5 ky B.P. (*6*). This suggests that although the sea-ice–poor TPD reached Greenland, American wood was landed on Ellesmere by an isolated BG (Fig. 2B). In the context of today's climate, a weak and isolated BG in combination with a strong TPD is associated with a positive Arctic Oscillation (AO) index, which is a situation with low pressure over the Arctic and high pressure over mid-latitudes, strong zonal winds, and fast passage of Siberian sea ice across the Arctic Ocean while American ice is retained in the BG (Fig. 2B) (*11*, *23*, *24*). Our results indicate that this situation may have prevailed during the HTM. At ~6 ky B.P., cooling sets in, as seen from the termination of beach ridge formation in the northern areas. In spite of the shortened open-water season, multiyear sea ice and driftwood in Greenland increased drastically. The amount of spruce also increased, showing that a steady export of ice from the BG had begun. We suggest that the cooling was accompanied by more frequent AO-negative situations with a stronger BG and weaker TPD. This is seen also in the accretion of ice shelves at the coast of Ellesmere Island (*5*), implying reduced wind stress. At ~2.5 ky B.P., the climatic cooling passed yet another threshold. The coast of North Greenland was now beleaguered by year-round sea ice, but on a centennial scale, periods with permanent land-fast ice changed with periods with large amounts of multiyear pack ice. The large amounts of wood brought in during these periods indicate that driftwood and multiyear sea ice reached their Holocene maximum, but the changing amounts of spruce and larch show that ice drift routes had become more variable than earlier.

In general, our sea-ice record for North Greenland follows the Holocene climate development, with an early warm period followed by declining temperatures, which were punctuated by relatively warmer and colder intervals (*17*, *25*). The reduction of the HTM sea ice in northern Greenland fits with the simulated ice distribution and surface temperature in orbitally forced ECHAM5/JSBACH/MPI-OM (EJM) and LOVECLIM general circulation climate model simulations (*3*, *4*, *10*). A tentative first approximation of the large-scale changes associated with the observed ice retreat north of Greenland can be obtained by selecting among the numerical experiments performed with the LOVECLIM model those that are the most similar to our observations [experiments E3 to E5 (*3*) and fig. S3]. In this exercise, our records would correspond in the model to an Arctic Ocean sea-ice cover in summer at 8 ky B.P. that was less than half of the record low 2007 level. The general buildup of sea ice from ~6 ky B.P. agrees with the LOVECLIM model, showing that summer sea-ice cover, which reached its Holocene maximum during the LIA, attained its present (~2000) extent at ~4 ky B.P. (fig. S3). However, despite the similarities at large scale and the long-term trends between model and observations, the complementarity in sea-ice abundance between East (Ellesmere) and West (Greenland), which is seen especially during the HTM, is not simulated in the climate models. The largest reduction in the EJM is indeed seen in the eastern part of the Arctic in association with an enhanced oceanic circulation and net northward heat transport (*4*). However, there are no signs in the EJM or in LOVECLIM of a concurrent simulated increase in the West. It has been seen in recent years that there is a strong influence on the sea-ice variability from the large-scale atmospheric flow anomalies and associated wind stress (*1*, *2*, *23*, *24*), and the importance of wind-stress is also known from basic sea-ice physics. Thus, it is likely that the model deficits are related to a too-weak large-scale AO-type flow response to the orbital forcing during the HTM. Such troubles in reproducing past sea-ice variations may also have an impact on future simulated regional changes using the same models. Therefore, improved understanding of these inconsistencies is important.

References and Notes

1. Arctic Monitoring and Assessment Programme, *AMAP 2009 Update on Selected Climate Issues of Concern* (Arctic Monitoring and Assessment Programme, Oslo, 2009).
2. M. C. Serreze, M. M. Holland, J. Stroeve, *Science* **315**, 1533 (2007).
3. H. Goosse, E. T. Driesschaert, T. Fichefet, M. F. Loutre, *Clim. Past* **3**, 683 (2007).
4. N. Fischer, J. H. Jungclaus, *Clim. Past* **6**, 155 (2010).
5. J. H. England *et al.*, *Geophys. Res. Lett.* **35**, L19502 (2008).
6. A. S. Dyke, J. England, E. Reimnitz, H. Jetté, *Arctic* **50**, 1 (1997).
7. L. Polyak *et al.*, *Quat. Sci. Rev.* **29**, 1757 (2010).
8. A. Häggblom, *Geogr. Ann. A* **64**, 81 (1982).
9. P. Wadhams, *Ice in the Ocean* (Gordon and Breach, London, 2000).
10. Information on materials and methods is available on *Science* Online.
11. I. G. Rigor, J. M. Wallace, R. L. Colony, *J. Clim.* **15**, 2648 (2002).
12. V. Pavlov, O. Pavlova, R. Korsnes, *J. Mar. Syst.* **48**, 133 (2004).
13. O. Eggertsson, *Arctic* **47**, 128 (1994).
14. R. W. G. Carter, *Coastal Environments* (Academic Press, London, 2002).
15. N. Reeh, *Sediment. Geol.* **165**, 333 (2004).
16. N. K. Larsen *et al.*, *Quat. Sci. Rev.* **29**, 3399 (2010).
17. D. S. Kaufman *et al.*, *Quat. Sci. Rev.* **23**, 2059 (2004).
18. C. Andersen, N. Koç, A. Jennings, J. T. Andrews, *Paleoceanography* **19**, PA2003 (2004).
19. A. E. Jennings, K. L. Knudsen, M. Hald, C. V. Hansen, J. T. Andrews, *Holocene* **12**, 49 (2002).
20. J. T. Andrews *et al.*, *Holocene* **19**, 71 (2009).
21. M. Ślubowska-Woldengen *et al.*, *Quat. Sci. Rev.* **26**, 463 (2007).
22. D. A. Darby, J. F. Bischof, *Paleoceanography* **19**, PA1027 (2004).
23. I. G. Rigor, J. M. Wallace, *Geophys. Res. Lett.* **31**, L09401 (2004).
24. J. E. Overland, M. Wang, *Tellus* **62A**, 1 (2010).
25. D. S. Kaufman *et al.*, Arctic Lakes 2k Project Members, *Science* **325**, 1236 (2009).
26. Greenland Ice Chart 1999–2009 (Danish Meteorological Institute, Copenhagen, Denmark); available at www.dmi.dk/dmi/index/gronland/iskort.htm.
27. P. J. Reimer *et al.*, *Radiocarbon* **51**, 1111 (2009).
28. C. B. Ramsey, *Quat. Sci. Rev.* **27**, 42 (2008).

Acknowledgments: The field work was funded mainly by the Danish Research Council (FNU) and the Commission for Scientific Research in Greenland (KVUG) with grants to S.F. and K.K. Logistic planning and support came from the Danish Polar Centre. P.M. and N.K.L. thank the Swedish Research Council (VR) for financial support and the Swedish Polar Research Secretariat for logistic support. A.L. thanks the Norwegian Research Council (SciencePub) and the Geological Survey of Norway for support. H.G. is a Research Associate with the Fonds National de la Recherche Scientifique (F.R.S.-FNRS-Belgium). N. Fischer of the Max Planck Institute for Meteorology provided sea-level pressure maps (see supporting online material).

Supporting Online Material

www.sciencemag.org/cgi/content/full/333/6043/747/DC1
Materials and Methods
SOM Text
Figs. S1 to S3
Tables S1 to S3
References

11 January 2011; accepted 14 June 2011
10.1126/science.1202760